EQUILIBRIUM, STABILITY AND EVOLUTION OF ELASTIC PLATES UNDER THE COMBINED EFFECTS OF STRESS AND SURFACE DIFFUSION

by ANDREW N. NORRIS[†]

(Department of Mechanical and Aerospace Engineering, Rutgers University, 98 Brett Road, Piscataway, New Jersey 08854-8058, USA)

[Received 18 April 1998]

Summary

The particles in an elastic plate are permitted to move by a surface diffusion process subject to the constraint that the total free energy does not increase. The static equilibrium, the quasi-static linear stability, and the quasi-static nonlinear evolution of the surface are examined under different loading conditions: tensile/compressive or flexural. The equilibrium configurations are such that the surface value of the chemical potential is constant, and their shapes depend upon the relative magnitude of elastic to surface energies. A linear stability analysis indicates that antisymmetric perturbations to the surface profile of a flat plate are most unstable for tensile loading and symmetric perturbations display the greatest instability under flexure. A new model for nonlinear non-equilibrium mechanics of thin plates is described and analysed. The main feature is that the elastic energy at the surface is approximated by that of an equivalent thin plate in a state of uniaxial stress, even as the profile changes. Nonlinear evolution of a perturbed flat plate is illustrated by numerical solution. A crevice gradually develops in the plate, eventually leading to rapid rupture and breakage. Scaling analysis near the ultimate rupture indicates a simple spatial and temporal dependence.

1. Introduction

The competition between the stabilizing effects of surface tension (energy) and the destabilizing effect of stress driven diffusion of surface particles has been proposed as a mechanism for the early stages of stress corrosion cracking and surface roughening (1). The diffusion causes material rearrangement in which atoms search for surface sites of lower chemical potential, away from stress concentrations. This effect has been shown to be unstable to linear perturbation (2, 3, 4), indicating that flat strained surfaces are inherently unstable, and the instability is independent of the sign of the stress: compressive or tensile. The consequent nonlinear evolution of stressed elastic half-spaces has been examined by several authors (5, 6, 7). For example, Yang and Srolovitz (5) showed that the surface instability creates a groove which steadily sharpens as it deepens. The rate of growth of the groove increases until it appears to diverge. Based upon an extensive series of numerical studies, Yang and Srolovitz were able to show that the critical groove depth at which the growth rate diverges is in excellent agreement with linear fracture mechanics. In fact, they reproduced the Griffith fracture criterion on the basis of surface diffusion alone, with no adjustable parameters.

Experimental evidence for the stress-driven surface instability has been forthcoming, and it has been used to explain effects in diverse material configurations such as helium crystals (8), polymer

^{† (}norris@norris.rutgers.edu)

gels and crystals (9), and solid–solid interfaces. The instability can be caused by ion infiltration into the solid leading to large misfit strains, and also under conditions of anodic dissolution (10). Thus, Tappin *et al.* (9) observed periodic surface structure on Zr₃Al crystals undergoing anodic dissolution in electropolishing. They ascribed the formation of the surface morphology to absorbed H₂ and consequent misfit strains near the surface, which are relaxed by surface diffusion. The fact that the phenomenon is observed in a variety of material systems indicates that it can be an important mechanism for the early growth of surface structure. However, it is doubtful that it can be used to explain the late stages of, for instance, fatigue or corrosion-assisted cracking, or other phenomena for which dislocations are the dominant mechanism (11, 12).

In this paper we consider thin elastic plates which can change under the stress-driven diffusion of surface particles. We first consider the elastic stability and compare the results obtained with those for a half-space, in the limit of infinite thickness. We demonstrate that the condition for thin-plate stability is quite different from that for thick plates, and it can be understood in terms of a uniaxial stress approximation. In the second part of the paper the nonlinear equilibrium and non-equilibrium of thin plates is examined using the uniaxial approximation. This simplifies the problem considerably and permits semi-analytic solutions. In particular, we examine the late behaviour of a notch as it traverses the entire plate, similar to the half-space groove observed by Yang and Srolovitz (5) but susceptible to analytic description. Both tensile/compressive and flexural loadings are considered. We begin with the general formulation of surface diffusion under applied stress.

2. The surface growth equation

Consider an elastic body V with traction-free surface S, under some state of applied loading. We will later examine in detail the example of a plate of infinite extent in two directions, in which case the surface comprises the top and bottom plate faces. The general phenomenon of surface instability is governed by the reduction in the total free energy,

$$\mathcal{E} = E - W,\tag{1}$$

comprising the work of applied loads, W, and the stored energy E made up of bulk elastic and surface energies:

$$E \equiv E_{\text{elastic}} + E_{\text{surface}},$$
 $E_{\text{elastic}} = \int_{V} dV U,$ $E_{\text{surface}} = \int_{S} dS \gamma,$ (2)

where U and γ are the volumetric and surface energy densities, respectively. If the surface is changing, with normal velocity c (positive is out of the material) then the rates of change of these energies are

$$\frac{dE_{\text{elastic}}}{dt} = \int_{S} dS \, cU, \qquad \frac{dE_{\text{surface}}}{dt} = -\int_{S} dS \, \gamma \, c\kappa. \tag{3}$$

Here, κ is the sum of the principal surface curvatures.* Thus, the total free energy satisfies

$$\frac{d\mathcal{E}}{dt} = \int_{\mathcal{S}} dS \, c\mu, \qquad \text{where } \mu \equiv U - \gamma \kappa, \tag{4}$$

and μ is known as the surface chemical potential. It is identically the energy required to add one volumetric unit[†] of material to the surface: U represents the additional energy required to coherently

^{*} Curvature is such that, for example, a solid sphere of radius a has $\kappa = -2/a$.

[†] The chemical potential is usually defined as the energy per atom or the energy per mole, in which case μ is multiplied by the atomic or molar volume, as the case may be.

match the new solid to the strained surface, and $(-\gamma\kappa)$ is the energy associated with creating new surface area. The precise form of the chemical potential is obtained by performing a *material* variation of the surface, and it is possible to represent μ in different ways, for example, by means of the Eshelby tensors for the bulk and for the surface (13).

ELASTIC PLATES

The change in the surface shape is assumed to be caused solely by the relative movement of particles, with total mass remaining the same. Assuming a constant density ρ_0 , this implies that

$$\frac{d}{dt} \int_{V} dV \, \rho_0 = \int_{S} dS \, \rho_0 c = 0. \tag{5}$$

(The assumption of constant density is consistent with the use of Lagrangian (or material) coordinates and with conservation of volume in these coordinates.) The mass conservation identity (5) is automatically satisfied if c is of the form (14)

$$c = -\operatorname{div}_{s}\mathbf{q},\tag{6}$$

where div_s denotes the surface divergence operator, and \mathbf{q} is a surface flux vector. Substitution into (4), and integration by parts (subject to appropriate boundary conditions) implies that

$$\frac{d\mathcal{E}}{dt} = \int_{S} dS \, \mathbf{q} \cdot \nabla_{s} \mu. \tag{7}$$

A physically realistic process will reduce the free energy, and this is guaranteed by (7) if the surface flux is proportional to the gradient of the chemical potential:

$$\mathbf{q} = -D_0 \nabla_s \mu, \qquad D_0 > 0, \tag{8}$$

which implies that

$$\frac{d\mathcal{E}}{dt} = -D_0 \int_{\mathcal{S}} dS \left(\nabla_s \mu \right)^2 \leqslant 0. \tag{9}$$

Generally, the energy will always decrease under rearrangement for any D_0 in the form of a positive definite second-rank surface tensor; however, here we restrict attention to isotropic surface diffusion.* Equations (6) and (8) give the surface velocity as

$$c = D_0 \nabla_s^2 \mu \,. \tag{10}$$

This is the central equation governing the surface growth. It is nonlinear because of the presence of the surface curvature in μ , and non-local because it involves determining the local variation in the strain energy, U. The appearance of U requires solving a separate static elastic problem for the stress and strain, σ_{ij} and ϵ_{ij} , which depends upon the global nature of the structure. For the sake of simplicity we take U as that of a linearly elastic material,

$$U = \frac{1}{2}\sigma_{ij}\epsilon_{ij},\tag{11}$$

where σ_{ij} and ϵ_{ij} are linearly related to one another. The elasticity problem is then linear but it involves a changing domain, and therein lies the greatest complication.

^{*} D_0 may be identified physically as (15) $D_0 = D_s n_s \Omega/(kT)$, where D_s is a surface diffusivity, n_s the surface number density of atoms capable of diffusing, Ω is the volume of a single atom, and kT is the temperature normalized by Boltzmann's constant

2.1 Linear stability analysis

A first attempt at understanding (10) is to linearize about an initial state, which we take as a flat surface for simplicity. Let $h(\mathbf{x}_s,t)$ be the time dependent perturbation to the surface, representing the increment in the thickness normal to the original flat surface, where \mathbf{x}_s lies on the flat surface. Thus, within the linear approximation, $\kappa = \nabla_{\perp}^2 h$, and $c = \partial h/\partial t$, where ∇_{\perp} represents the gradient operator on the fixed, flat surface. The strain energy term U is linearized about its initial state by assuming that the total stress and strain are the sum of initial values $\sigma_{ij}^{(0)}$ and $\epsilon_{ij}^{(0)}$, plus those arising from the surface perturbation. Thus $\sigma_{ij} = \sigma_{ij}^{(0)} + \sigma_{ij}^{(1)}$ and $\epsilon_{ij} = \epsilon_{ij}^{(0)} + \epsilon_{ij}^{(1)}$, where the initial stress $\sigma_{ij}^{(0)}$ is in equilibrium with zero traction on the flat surface, but it is not necessarily homogeneous within the body. We include this possibility to allow for the important case of a beam in flexure, which we analyse later.

The perturbed surface stress and strains can be evaluated using the condition that the modified surface is traction free. Linearizing the zero traction condition $\sigma_{ij}^{(0)} n_j = 0$ about the unperturbed flat configuration implies the following traction condition:

$$\sigma_{ij}^{(0)} n_j^{(0)} + \sigma_{ij}^{(1)} n_j^{(0)} - \sigma_{i\alpha}^{(0)} h_{,\alpha} + \left[\mathbf{n}^{(0)} . \nabla \sigma_{ij}^{(0)} \right] n_j^{(0)} h = 0 \qquad \text{on the unperturbed surface.} \tag{12}$$

Here, $h_{,\alpha}$, $\alpha=1$, 2, denotes the components of the surface gradient of h. The first term in (12) vanishes because the initial stress is traction free on the surface, that is, $\sigma_{ij}^{(0)} n_j^{(0)} = 0$. The final term can be simplified using the equilibrium equations, $\sigma_{ij,j}^{(0)} = 0$, to give $\left[\mathbf{n}^{(0)} \cdot \nabla \sigma_{ij}^{(0)}\right] n_j^{(0)} = -\sigma_{i\alpha,\alpha}^{(0)}$ so that the perturbed stress satisfies

$$\sigma_{ij}^{(1)} n_i^{(0)} = \left(\sigma_{i\alpha}^{(0)} h\right)_{,\alpha} \qquad \text{on the unperturbed surface.} \tag{13}$$

The perturbed strain $\epsilon_{ij}^{(1)}$ is therefore a linear functional of h, obtained by solving the boundary-value problem defined by (13), supplemented by the equilibrium equations $\sigma_{ij,j}^{(1)} = 0$ within the body. In general, this solution represents the surface values of $\epsilon_{ij}^{(1)}$ as a non-local surface operator acting on h, the precise form of which depends on the geometry of the body and its surface. It is interesting to note that if the initial stress is homogeneous (constant) on the surface then the non-zero stresses indicated in equation (13) are tangential or shear stresses only.

The perturbed surface energy is

$$\delta U = \delta U_1 + \delta U_2,\tag{14}$$

where U_1 is the linear change associated with $\sigma_{ij}^{(1)}$ and $\epsilon_{ij}^{(1)}$, which follows from (11) as

$$\delta U_1 = \sigma_{ij}^{(0)} \epsilon_{ij}^{(1)} = \epsilon_{ij}^{(0)} \sigma_{ij}^{(1)}. \tag{15}$$

The second term δU_2 arises from the possible variability of the initial stress and strain near the surface:

$$\delta U_2 = h \, \mathbf{n}^{(0)} . \nabla U = h \, \epsilon_{ij}^{(0)} \, \mathbf{n}^{(0)} . \nabla \sigma_{ij}^{(0)}. \tag{16}$$

The linearized growth equation is then

$$\partial h/\partial t = D_0 \,\nabla_{\perp}^2 \left(\sigma_{ij}^{(0)} \epsilon_{ij}^{(1)} + h \,\epsilon_{ij}^{(0)} \,\mathbf{n}^{(0)} \cdot \nabla \sigma_{ij}^{(0)} - \gamma \,\nabla_{\perp}^2 h\right). \tag{17}$$

Before analysing the specific implications of this equation, it is evident from (17) that the linear

ELASTIC PLATES 287

stability of a surface depends on three factors: the surface energy γ , the surface stress $\sigma_{ij}^{(0)}$, and the normal derivative of the initial stress. The first two are well known and have been considered many times before in the literature, see for example, (14). The curvature term is local and always acts as a stabilizing influence, whereas the stress term is non-local but leads to instability. It is also clear that the effect of the stress term $\sigma_{ij}^{(0)} \epsilon_{ij}^{(1)}$ is independent of the sign of the initial stress $\sigma_{ij}^{(0)}$ since the perturbed strain is linearly proportional to this via the boundary condition (13). The appearance of the normal derivative of the initial stress in the linear growth equation (17) is significant, but has not been previously considered in the literature. We note that it is a local effect which can be either destabilizing or stabilizing, depending as $\mathbf{n}^{(0)}.\nabla U^{(0)}$ is positive or negative, respectively, where $U^{(0)}$ is the initial strain energy.

It remains to represent the perturbed surface strain $\epsilon_{ij}^{(1)}$ in terms of the perturbation h, which depends upon the global static elasticity problem. The case of a plate in a state of plane strain is considered in detail next.

3. Stability of a plate in plane strain

3.1 Unilateral perturbations

The plate has initial thickness 2a with centre plane $x_3 = 0$ and extends to infinity in the (x_1, x_2) -plane. We consider plane-strain deformation in the (x_1, x_3) -plane, both for the initial state of stress and for the perturbation. We first assume that the perturbation in thickness is confined to the side $x_3 = a$, and is such that the deformed plate has thickness 2a + h, where h is sinusoidal in x_1 of wavenumber k:

$$h = h_0(t)\sin kx_1. \tag{18}$$

The driving force of the perturbation on $x_3 = a$ is the uniaxial in-surface stress:

$$\sigma_{ij}^{(0)}(x_1, a) = \sigma_0 \,\delta_{i1} \delta_{j1},\tag{19}$$

where σ_0 is the value of the in-surface stress. This is assumed constant, independent of x_1 and t. However, the initial stress is not necessarily independent of x_3 as one goes into the material. We consider the possibility that it may vary as*

$$\frac{\partial \sigma_{ij}^{(0)}}{\partial x_3}(x_1, x_3) \bigg|_{x_3 = a} = \frac{\sigma_0}{b} \, \delta_{i1} \delta_{j1},\tag{20}$$

where b is a constant, positive or negative although zero is precluded as being unphysical.

Note that only the surface value of $\epsilon_{11}^{(1)}$ is required in the growth equation (17). The boundary-value problem for $\epsilon_{ij}^{(1)}$ is

$$\sigma_{i3}^{(1)}(x_1, a, t) = \sigma_0 k h_0(t) \cos k x_1, \tag{21}$$

$$\sigma_{i3}^{(1)}(x_1, -a, t) = 0,$$
 (22)

supplemented by the equilibrium equations. The solution to this plane strain boundary-value

^{*} If the initial stress has only the single component $\sigma_{11}^{(0)}(x_1, x_3)$ which is independent of x_1 , then $\sigma_{11} = \sigma_0 (1 + x_3/b)$ is consistent with the compatibility equation $\nabla^2 \sigma_{11} = 0$.

problem can be found using the Airy stress function method (16), and we omit the details. The main result is

$$\epsilon_{11}^{(1)}(x_1, \pm a, t) = -\frac{\sigma_0}{E_p} kh(x_1, t) \left[\frac{1}{\tanh ka + \frac{ka}{\cosh^2 ka}} \pm \frac{1}{\coth ka - \frac{ka}{\sinh^2 ka}} \right], \quad (23)$$

where E_p is the plane-strain modulus, $E_p = E/(1 - v^2)$, with E and v the Young's modulus and Poisson's ratio, respectively. The variation in the strain energy is thus

$$\delta U = 2U h(x_1, t) \left[\frac{1}{b} - k f(ka) \right], \tag{24}$$

where $U = \sigma_0^2/(2E_p)$ and

$$f(\xi) = \frac{1}{\tanh \xi + \frac{\xi}{\cosh^2 \xi}} + \frac{1}{\coth \xi - \frac{\xi}{\sinh^2 \xi}}.$$
 (25)

The growth equation (17) now reduces to a simple ordinary differential equation for $h_0(t)$:

$$\frac{dh_0}{dt} = D_0 \left[\frac{\sigma_0^2}{E_p} \left(k^3 f(ka) - \frac{k^2}{b} \right) - \gamma k^4 \right] h_0(t) . \tag{26}$$

The solution is of the form $h_0(t) = h_0(0) \exp(\eta t)$, where the growth rate of the perturbation depends upon the sign of the quantity

$$\eta = \frac{D_0 \gamma}{a} k^3 \left[\Lambda \left(f(ka) - \frac{1}{kb} \right) - ka \right],\tag{27}$$

and Λ is a non-dimensional ratio of strain energy to surface tension,

$$\Lambda = \frac{\sigma_0^2 a}{\gamma E_p} \,. \tag{28}$$

The perturbation (18) is stable (unstable) if $\eta < 0$ (> 0), where $\eta = \eta(\Lambda, a/b, ka)$ is given by (27). Some understanding of the regions of stability can be obtained from the asymptotic properties of $f(\xi)$:

$$f(\xi) = \begin{cases} 2/\xi + \frac{8}{15}\xi + O(\xi^3), & \xi \ll 1, \\ 2 + O(\xi e^{-2\xi}), & \xi \gg 1. \end{cases}$$
 (29)

If a/b < 2 it follows that there is a range of k beginning at 0 for which the perturbation is unstable for any value of Λ . Thus, a/b = 2 presents a critical value demarcating configurations* which always exhibit instability (a/b < 2) from those which display instability only if Λ exceeds a

^{*} A referee suggests the helpful terminology 'large flexure' for a/b > 2, and 'small flexure' for a/b < 2.

Table 1 The asymptotic values of k_0a , $k_{\text{max}}a$ and η_{max} for large and small Λ , assuming that a/b < 2

| | $ \Lambda \ll 1 $ $ a/b = 0 $ | $ \Lambda \ll 1 $ $ a/b = 1 $ | Λ ≫ 1 |
|--|-------------------------------|-------------------------------|--------------------------|
| k_0a | $\sqrt{2\Lambda}$ | $\sqrt{\Lambda}$ | 2Λ |
| $k_{\max}a$ | $\sqrt{\Lambda}$ | $\sqrt{\frac{1}{2}\Lambda}$ | $\frac{3}{2}\Lambda$ |
| $rac{a^4}{D_0 \gamma} \eta_{ m max}$ | Λ^2 | $\frac{1}{4}\Lambda^2$ | $\frac{27}{16}\Lambda^4$ |

positive value, Λ_c , which depends upon a/b (> 2). This result can be understood in terms of energy accountancy: if the energy near the stress-free surface increases rapidly enough in the normal direction (a/b > 2), then it is more difficult to lower the total free energy of the system by means of perturbing the surface, regardless of the surface tension γ . Conversely, rearrangement of particles near the surface is more likely if the strain energy decreases in the normal direction near the surface (a/b < 2).

In summary, the perturbation (18) is stable for all wavenumbers if $a/b \ge 2$ and $\Lambda \le \Lambda_c$. For a/b = 2 the critical value is $\Lambda_c \approx 15/8$, from equation (29), and as $a/b \to \infty$ the critical value tends to $\Lambda_c \approx a/b \gg 1$. For a/b > 2 and $\Lambda > \Lambda_c$ there is a range of ka for which $\eta > 0$. Conversely, if a/b < 2 then for any value of Λ there is a unique positive value of ka at which η achieves a positive maximum.

Let us now examine in detail the case when destabilization is possible for any Λ , that is, $-\infty < a/b < 2$. First, there is a positive value of ka at which η is zero, say $k_0a = \xi_0$, where ξ_0 is the root of $\Lambda(f(\xi) - a/(b\xi)) = \xi$. The surface perturbation is stable $(\eta < 0)$ if k exceeds this value and unstable $(\eta > 0)$ otherwise. The maximal instability occurs when the growth rate is largest, which occurs at the wavenumber $k_{\max}a = \xi_{\max}$, $0 < \xi_{\max} < \xi_0$, at which $\Lambda(\xi^3 f(\xi) - (a/b)\xi^2) - \xi^4$ achieves a maximum. There are two distinct types of behaviour, depending as Λ is small or large, which can be understood from the asymptotic form of $f(\xi)$ in (29). For small Λ we consider the two cases of $b = \infty$ (no normal variation in the surface stress) and b = a (flexure) to obtain the results in Table 1.

Figure 1 shows the ratio $k_{\rm max}/k_0$ versus Λ for a/b=0. The ratio as plotted takes the asymptotic values of $1/\sqrt{2}$ for $\Lambda<\frac{1}{2}$ and $\frac{3}{4}$ for $\Lambda>2.5$, respectively. Hence, Fig. 1 indicates that the asymptotic approximations of Table 1 are adequate for $\Lambda<\frac{1}{2}$ or $\Lambda>2.5$.

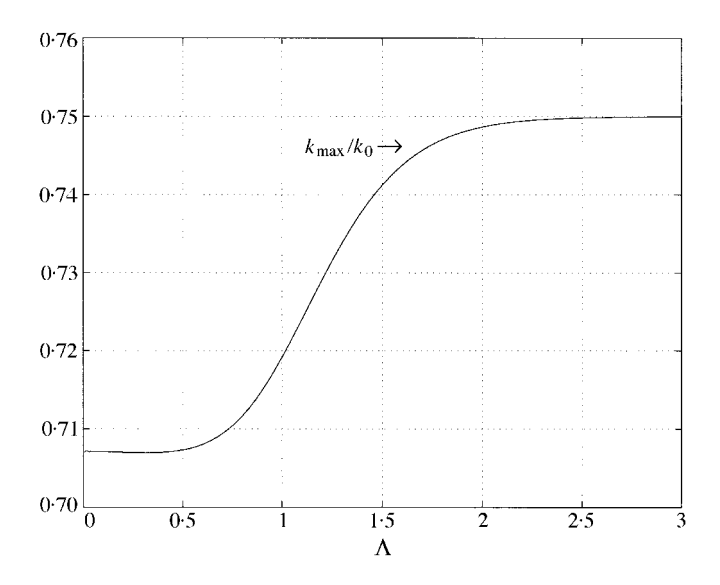


Fig. 1 The ratio k_{max}/k_0 versus Λ for a/b=0, indicating that the asymptotic estimates of Table 1 are reasonable outside the range $\frac{1}{2} < \Lambda < 2.5$

3.2 Half-space and thin-plate limits

The present results contain the limit of an elastic half-space as the special case of finite kb for $\Lambda \to \infty$:

$$\eta = D_0 \gamma \left[\frac{\sigma_0^2 k^3}{\gamma E_p} \left(2 - \frac{1}{kb} \right) - k^4 \right]$$
 for a half-space. (30)

The further limit $1/kb \rightarrow 0$ recovers the well-known results for the maximally unstable wavenumber of a uniformly stressed half-space (3), which are given by the right-hand column in Table 1, or equivalently,

$$k_{\text{max}} = \frac{3\sigma_0^2}{2\gamma E_p}$$
, $\eta_{\text{max}} = \frac{27D_0\sigma_0^8}{16\gamma^3 E_p^4}$ uniformly stressed half-space. (31)

For finite kb, the influence of b is to stabilize if b>0 and destabilize for b<0. For small but negative values of b such that $k|b|\ll 1$ the half-space acts like a thin plate of semi-thickness (-2b); see equation (33) below. That is, the non-uniformly stressed half-space with strain energy decreasing in the normal direction (b<0) has the same stability properties as a plate with a=-2b in a state of *uniform* uniaxial stress. Conversely, $\eta<0$ for all k if

$$\frac{1}{b} > \frac{\sigma_0^2}{\gamma E_p} \Leftrightarrow \text{half-space unconditionally stable.}$$
 (32)

The values of k_0 , k_{max} and η_{max} for the plate of semi-thickness a are, of course, independent of a in the half-space limit; see (31). However, Table 1 indicates that these parameters are strongly

dependent upon a and b for thin plates, $\Lambda \ll 1$. The thin-plate limit follows from (27) and (29)₁, as

$$\eta = D_0 \gamma \left[\frac{\sigma_0^2 k^3}{\gamma E_p} \left(\frac{2}{ka} - \frac{1}{kb} \right) - k^4 \right]$$
 for a thin plate. (33)

We find for instance that

$$k_{\text{max}} = \frac{\sigma_0}{\sqrt{a\gamma E_p}} \times \begin{cases} 1, & \eta_{\text{max}} = \frac{D_0 \sigma_0^4}{a^2 \gamma E_p^2} \times \begin{cases} 1, & a/b = 0, \\ \frac{1}{4}, & a/b = 1, \end{cases}$$
 for thin plates. (34)

These are to be compared with the well-known results for the homogeneously stressed half-space, given in (31). Comparison of the thin-plate (TP) parameters for a/b = 0 against those for the half-space (HS), yields

$$\frac{k_{\text{max}}^{(\text{TP})}}{k_{\text{max}}^{(\text{HS})}} = \frac{2}{3\Lambda^{\frac{1}{2}}}, \qquad \frac{\eta_{\text{max}}^{(\text{TP})}}{\eta_{\text{max}}^{(\text{HS})}} = \frac{16}{27\Lambda^{2}}.$$
 (35)

We see that the relative magnitudes depend upon the non-dimensional parameter Λ , which is a measure of the elastic strain energy per unit area of the plate surface ($\approx \sigma_0^2 a/E_p$) versus the surface energy (tension) per unit area (γ).

3.3 Symmetric and antisymmetric perturbations

The previous analysis assumed that one side of the plate is perturbed while the other remains unchanged. However, the existence of the two sides $x_3 = \pm a$ means that other types of perturbation involving simultaneous deformation of the two faces may be more or less stable than the unilateral perturbation. We consider the two special cases in which the plate deforms in such a manner that the additional material on the two sides is either the same, or the opposite. Let $h(x_1, t)$, given by (18), denote the additional material on $x_3 = +a$, then the symmetric (antisymmetric) perturbation is defined by the addition of h(-h) on the opposite side, $x_3 = -a$.

At the same time, we consider two physically significant states of initial stress: *tensile* and *flexural* loading, defined as follows.

Tensile loading:
$$\sigma_{ij}^{(0)}(x_1, \pm a) = \sigma_0 \, \delta_{i1} \delta_{j1}, \quad \frac{\partial \sigma_{ij}^{(0)}}{\partial x_3}(x_1, x_3) \bigg|_{x_3 = \pm a} = 0.$$
 (36)
Flexural loading: $\sigma_{ij}^{(0)}(x_1, \pm a) = \pm \sigma_0 \, \delta_{i1} \delta_{j1}, \quad \frac{\partial \sigma_{ij}^{(0)}}{\partial x_3}(x_1, x_3) \bigg|_{x_3 = \pm a} = \pm \frac{\sigma_0}{a} \, \delta_{i1} \delta_{j1}.$

The 'tensile' stress occurs under a state of uniaxial loading, and it may be either compressive or tensile, although we call it tensile for simplicity. The results reported here are independent of the sign of the initial stress: they depend only on the magnitude of the strain energy and its local variation. The flexural stress state is characteristic of a plate in bending with an internal stress which is approximately uniaxial, zero at the centre and varying linearly with x_3 such that

$$\sigma_0 = \frac{M_0 a}{I}$$
, where $I = \frac{2}{3} a^3$. (37)

Here, M_0 is the effective moment in the x_2 -direction acting on the cross-section $-a \le x_3 \le a$.

The stability of the symmetric and antisymmetric perturbations under the tensile and flexural initial loadings can be analysed by linearly superposing the previous results for the unilateral perturbation. The details of the procedure are not of interest except to note that the contribution to the growth equation from the stress variability $(1/b \neq 0)$ is evaluated only on the side at which the growth is being analysed. However, for both parities, symmetric and antisymmetric, the two faces grow so as to maintain parity, within the linear approximation of course. Thus, we find that the growth rates are

where $\xi = ka$ and $f_S(\xi)$ and $f_A(\xi)$ partition $f(\xi) = f_S(\xi) + f_A(\xi)$ as

$$f_S(\xi) = \frac{1}{\tanh \xi + \frac{\xi}{\cosh^2 \xi}}, \qquad f_A(\xi) = \frac{1}{\coth \xi - \frac{\xi}{\sinh^2 \xi}}.$$
 (39)

Using the asymptotic properties of f_S and f_A (that is, $f_S \approx 1/2\xi$, and $f_A \approx 3/(2\xi)$ as $\xi \to 0$; f_S , $f_A \to 1$ as $\xi \to \infty$, and $f_S < f_A$ for $0 < \xi < \infty$) it is clear that some of these configurations are more unstable than others for fixed values of Λ . Thus, for tensile loading, the antisymmetric perturbation is more unstable than the symmetric perturbation. Conversely, the symmetric perturbation is the more unstable of the two for flexural loading. In fact, since $2f_S(\xi) - 1/\xi = \frac{2}{3}\xi + O(\xi^2)$ for $\xi \to 0$, it follows that the antisymmetric perturbation of the flexurally loaded plate is linearly stable for all ka unless Λ exceeds approximately $\frac{3}{2}$.

Finally, we note that in the thin-plate limit $\xi \ll 1$, the growth rates for tensile and flexural symmetric perturbations follow from (38) as

$$\eta = \begin{cases}
D_0 \left[\frac{F_0^2 k^2}{4E_p a^3} - \gamma k^4 \right], & \text{tensile, symmetric, thin plate,} \\
D_0 \left[\frac{9M_0^2 k^2}{2E_p a^5} - \gamma k^4 \right], & \text{flexural, symmetric, thin plate.}
\end{cases}$$
(40)

The remainder of the paper discusses thin plates with large variations in thickness but which maintain symmetric profiles. The two predictions of (40) will serve as a check on the nonlinear theory.

4. Symmetric equilibrium configurations of thin plates

4.1 The uniaxial stress approximation

We now consider plates which are far from flat, and examine the possible equilibrium shapes of such plates under the combined influence of surface tension and elastic energy. When the former

effect is the only one present then the most favorable configuration of a material is well known to be spherical, the shape that minimizes surface area for a given volume. If we restrict the class of shapes to ones which are symmetric about the plane $x_3 = 0$ and that extend to infinity in both x_1 and x_2 then the flat plate is another equilibrium solution. We consider the analogous configurations of this type under the simultaneous influence of elastic energy and surface tension. That is, we look for surfaces symmetric about $x_3 = 0$ that extend to infinity in the other directions, and for simplicity, are also independent of the x_2 -coordinate. The search is therefore for uni-dimensional surfaces which are periodic in the x_1 -direction (The unit period is introduced only to reduce the problem to one on a finite domain, and the length of a period has nothing in common with the length of the periodic perturbations in section 3.) One reason why we restrict attention to plates that maintain their symmetry about the centre line is because these can still be treated using a relatively simple uniaxial stress theory: either membrane (tensile/compressive) or flexural, which will be explained below. Antisymmetric deformation leads to nonlinear mixing of these two simple modes of deformation, and will not be treated further here.

The equilibrium configurations that we will determine below do not have any particular stability properties. In fact, they will generally be linearly unstable to time dependent perturbation. However, if the diffusion process is relatively slow they can maintain their shape for a long time.

The equilibrium conditions are twofold. First, the absence of surface motion implies that the chemical potential μ must be constant, so that there is no motivation for surface diffusion (see (6)):

$$\mu = \mu_0$$
 on the surface. (41)

The second equilibrium condition is the usual elastic one: that the stress be divergence free within the body and give zero traction on the surface. In general, this requires solving a two-dimensional elasticity boundary-value problem, and then evaluating the strain energy U on the surface. For the remainder of the paper we take the simplifying step of replacing the strain energy by the equivalent strain energy as predicted by simple beam theory of elasticity. Two different types of loading are considered: tensile and flexural. Both of these lead to approximately uniaxial stress distributions for thin plates, so the present theory can be considered a thin-plate approximation.

The surface is defined by the rectangular material coordinates $x_1 \equiv x$ and $x_3 = \pm a(x, t)$. The strain energy at the surface is a function of the plate semi-thickness a(x, t) only, that is,

$$U = \bar{U}(a)$$
 at the surface. (42)

The function $\bar{U}(a)$ can be found by noting that the surface strain energy is $U = \sigma_{11}^2(a,t)/(2E_p)$, where $\sigma_{11}(a,t)$ is the value of the uniaxial stress at the surface. This is easily estimated for either tensile or flexural initial loading using 'strength of materials' concepts. Let F_0 be the effective force acting across any section in the x-direction, then $\sigma_{11} = F_0/2a$, and σ_{11} is actually constant across the section. Let M_0 be the effective bending moment in flexural loading, then σ_{11} varies linearly across the symmetric section, and according to (37), $\sigma_{11}(a,t) = 3M_0/(2a^2)$. Elimination of $\sigma_{11}^2(a,t)$ leads to the following expressions:

$$\bar{U}(a) = \begin{cases} F_0^2/(8E_p a^2) & \text{in tension,} \\ 9M_0^2/(8E_p a^4) & \text{in flexure.} \end{cases}$$
 (43)

Equation (43) is a direct consequence of the uniaxial approximation for the stress and it permits us to eliminate the stress as a variable. We have thus circumvented the problem of solving the static elasticity problem on a variable domain, and it remains to enforce (41).

4.2 Equilibrium shapes

The assumed symmetry about $x_3 = 0$ means that only the upper surface at $x_3 = a$ needs to be considered. Based upon the assumptions for the elastic energy, the chemical potential of (4) can be replaced by a function of a:

$$\mu = \bar{\mu}(a, a_{.x}, t) \equiv \bar{U}(a) - \gamma \kappa, \tag{44}$$

where the curvature is

$$\kappa = a_{.xx} / (1 + (a_{.x})^2)^{3/2}. \tag{45}$$

The surface equilibrium condition (41) therefore becomes

$$\bar{U}(a) - \gamma \kappa = \mu_0. \tag{46}$$

Note that the curvature can be rewritten as

$$\kappa = -\frac{d}{da} \frac{1}{\sqrt{1 + (a_x)^2}},\tag{47}$$

and hence (46) may be integrated to give

$$\int_{a_1}^a da \, \bar{U}(a) + \frac{\gamma}{\sqrt{1 + (a_{,x})^2}} - \mu_0 a = \frac{\gamma}{\sqrt{1 + (a_{,x})^2}} \bigg|_{a=a_1} - \mu_0 a_1 \tag{48}$$

for arbitrary a_1 .

The function $\bar{U}(a)$ is a monotonically decreasing function of a, and hence the strain energy is maximal at the thinnest section and minimal at the widest section of the plate. However, $\bar{U}(a)$ is always positive, and since the term $(-\gamma\kappa)$ must also be positive at the widest section* it follows that the constant chemical potential is positive:

$$\mu_0 > 0. \tag{49}$$

Another way of looking at it is that there must be a point of inflection, at which $\kappa = 0$ and hence μ_0 equals the (necessarily positive) strain energy at the point of inflection.

Let us choose the lower limit of integration in (48) to be the value at the thinnest section, at which the slope is zero, that is, $a_{,x} = 0$ at $a = a_1$, so that (48) becomes

$$\int_{a_1}^a da \, \bar{U}(a) + \frac{\gamma}{\sqrt{1 + (a_x)^2}} = \mu_0(a - a_1) + \gamma. \tag{50}$$

Similarly, let a_2 be the maximum semi-thickness, so that $0 < a_1 \le a \le a_2$. Then, equating a with the thickest section specifically, that is, $a = a_2$, equation (50) implies that

$$\int_{a_1}^{a_2} da \, \bar{U}(a) = \mu_0 \, (a_2 - a_1). \tag{51}$$

Hence, the independent parameters which define the problem may be taken as the minimum and

^{*} This implicitly assumes that the section is a C^1 continuously varying function of x, as opposed to C^0 with possible piecewise smooth slope.

maximum thicknesses, in terms of which the constant chemical potential is the thickness averaged value of the strain energy:

$$\mu_0 = \frac{1}{a_2 - a_1} \int_{a_1}^{a_2} da \, \bar{U}(a). \tag{52}$$

Also, equation (50) provides an ordinary differential equation for the surface profile,

$$\frac{da}{dx} = \pm \left[\frac{1}{(1 - G(a))^2} - 1 \right]^{\frac{1}{2}},\tag{53}$$

where G(a) is

$$G(a) = \frac{1}{\gamma} \int_{a_1}^a da \left[\bar{U}(a) - \mu_0 \right] = \frac{1}{\gamma} \left\{ \int_{a_1}^a da \, \bar{U}(a) - \left(\frac{a - a_1}{a_2 - a_1} \right) \int_{a_1}^{a_2} da \, \bar{U}(a) \right\}. \tag{54}$$

Note that the function G satisfies

$$G(a_1) = 0$$
, $G(a_2) = 0$, and $G(a) > 0$ for $a_1 < a < a_2$. (55)

Hence, for a given value of the surface tension there is a limit on the range of possible a_1 and a_2 for which equilibrium profiles exist. Specifically, (53) implies that the maximum value of G(a) cannot exceed unity. From its definition in (54), and using the identity (52), we see that the maximum value of G occurs at the point of inflection of the surface, where $\kappa = 0$ and $a = a_0$ such that

$$\bar{U}(a_0) = \mu_0. \tag{56}$$

It is not possible to evaluate a_0 and $G(a_0)$ in general; however, for the two cases of concern, in (43), we can determine all the necessary parameters.

Let σ_0 be the value of the surface stress at the point of inflection $a=a_0$, that is $\sigma_0=F_0/(2a_0)$ for tension, and $\sigma_0=3M_0/(2a_0^2)$ for flexure. Define the non-dimensional parameter Λ_0 , by analogy with the non-dimensional parameters for the flat plate in (28),

$$\Lambda_0 = \frac{\sigma_0^2 a_0}{\gamma E_p}.\tag{57}$$

It then follows from the identity (56) that for either type of loading we have

$$\Lambda_0 = \frac{2\mu_0 a_0}{\gamma}.\tag{58}$$

This is a useful parameter with which to represent G(a) and other quantities; thus

Tension:
$$a_0^2 = a_1 a_2$$
, $G(a) = \Lambda_0 \frac{(a_2 - a)(a - a_1)}{2aa_0}$,
Flexure: $a_0^4 = \frac{3(a_2 - a_1)}{1/a_1^3 - 1/a_2^3}$, $G(a) = \frac{\Lambda_0}{4a_0} \left[a_1 + a_2 - 2a + \left(\frac{1}{a_1^3} + \frac{1}{a_2^3} - \frac{2}{a^3} \right) \frac{(a_2 - a_1)}{1/a_1^3 - 1/a_2^3} \right]$. (59)

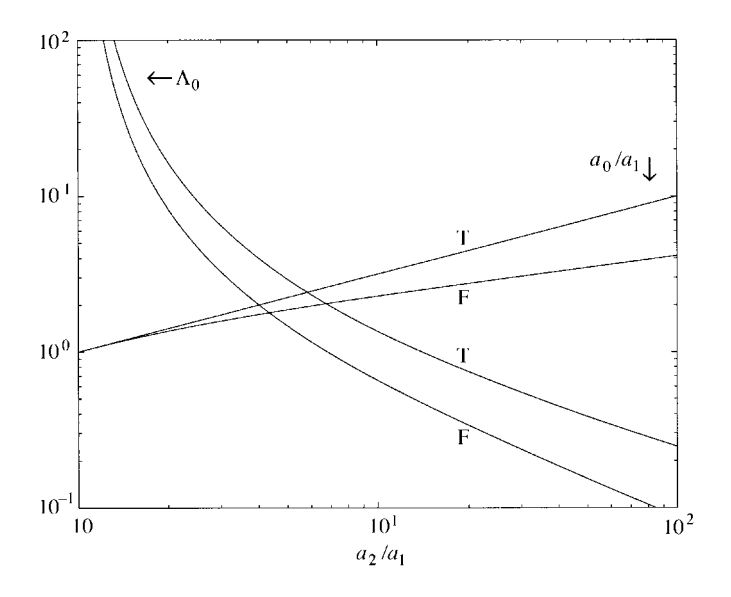


Fig. 2 The two sets of curves show (i) the values of a_0/a_1 versus a_2/a_1 for tensile (T) and flexural (F) loading, from equations (59), and (ii) the maximum permissible values of Λ_0 allowed under the constraint (60)

The constraint

$$G(a_0) < 1 \tag{60}$$

can now be evaluated for each type of loading. For the plate in tension, equation (60) implies that

$$\Lambda_0 < 2 / \left[\left(\frac{a_2}{a_1} \right)^{\frac{1}{4}} - \left(\frac{a_1}{a_2} \right)^{\frac{1}{4}} \right]^2. \tag{61}$$

Figure 2 shows plots of the maximum possible values of Λ_0 . For a given value of a_2/a_1 , there is a range of Λ_0 , bounded above by the curves in Fig. 2, for which symmetric equilibrium configurations exist. Figure 2 also shows a_0/a_1 versus a_2/a_1 for the two types of loading. This indicates where the point of inflection lies relative to a_1 and a_2 , and $a=a_0$ is also the point on the surface at which the strain energy equals μ_0 .

4.3 Examples of plates in equilibrium

The equilibrium shapes can be determined from (53) by quadrature. Only one sign of the right member needs to be considered, the solution for the other follows by symmetry arguments. Thus, let x = 0 at $a = a_1$, the 'neck' of the plate, then we evaluate x as a function of a:

$$x = \int_{a_1}^{a} da \left[\frac{1}{\left(1 - G(a)\right)^2} - 1 \right]^{-\frac{1}{2}}, \qquad a_1 \leqslant a \leqslant a_2.$$
 (62)

The integral has integrable singularities at the two limits a_1 and a_2 , but they can be rendered

ELASTIC PLATES 297

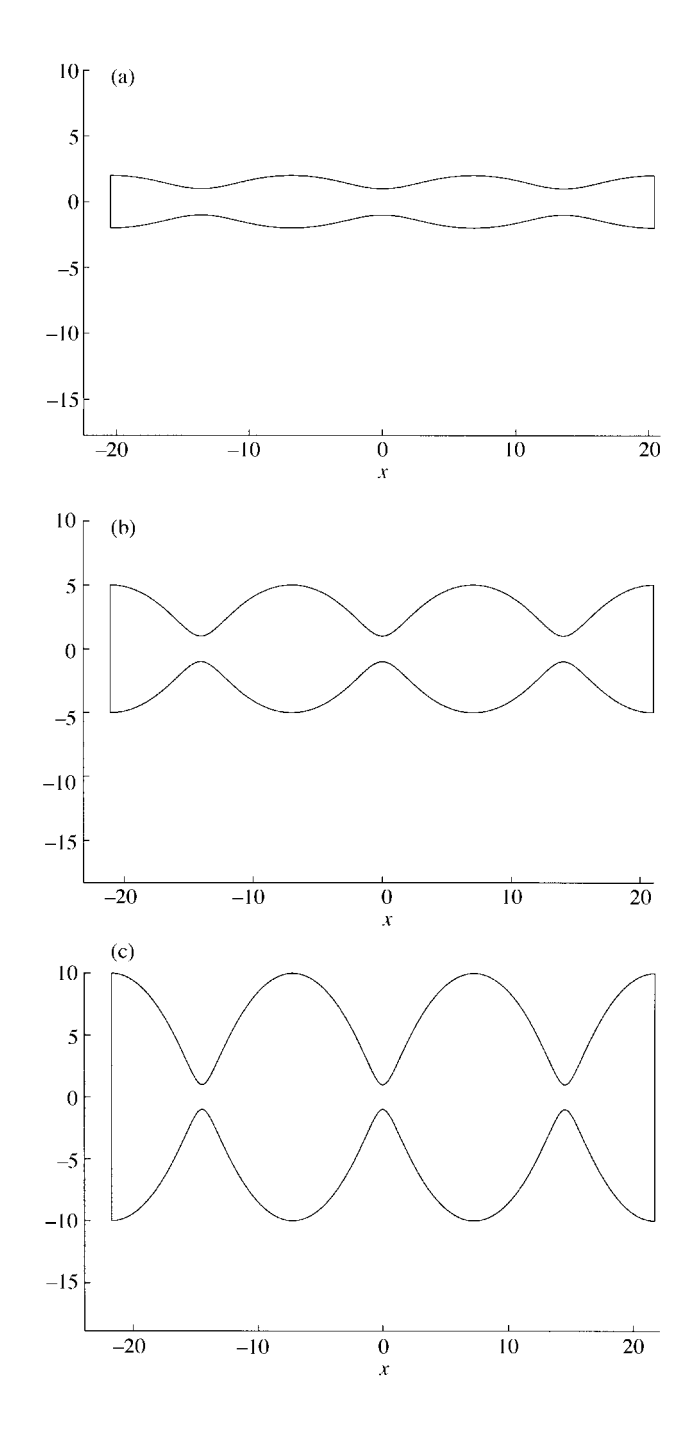


Fig. 3 The equilibrium shapes for tensile loading. The curves show the upper and lower surfaces of three periods of the basic shape. (a) $a_2/a_1=2$, $\Lambda_0=1.6484$; (b) $a_2/a_1=5$, $\Lambda_0=0.2927$; (c) $a_2/a_1=10$, $\Lambda_0=0.1353$. In each case Λ_0 is chosen to make $G(a_0)=0.1$

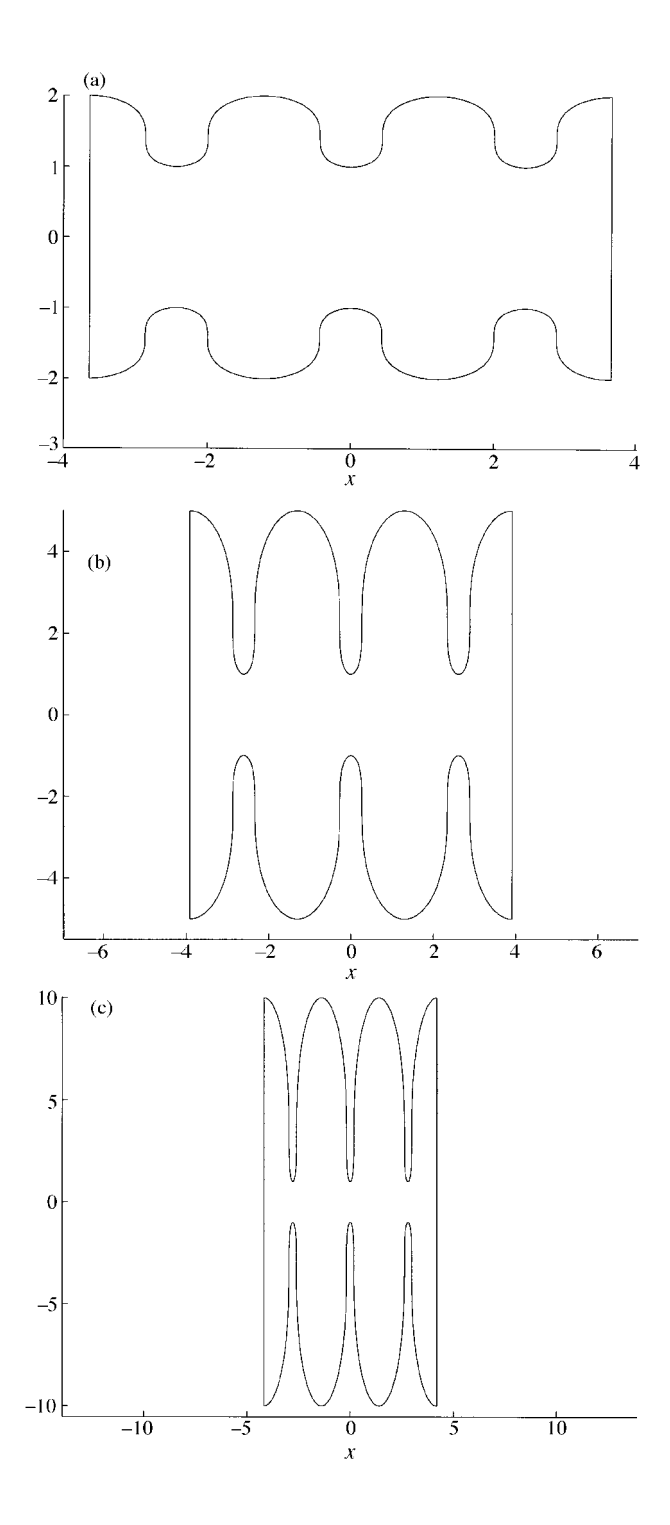


Fig. 4 The equilibrium shapes under tensile loading for the same parameters as in Fig. 3, except that Λ_0 is chosen to make $G(a_0)=1$, the maximum permissible value, that is, they are 10 times the values in Fig. 3. (a) $a_2/a_1=2$, $\Lambda_0=16\cdot4836$; (b) $a_2/a_1=5$, $\Lambda_0=2\cdot9268$; (c) $a_2/a_1=10$, $\Lambda_0=1\cdot3526$

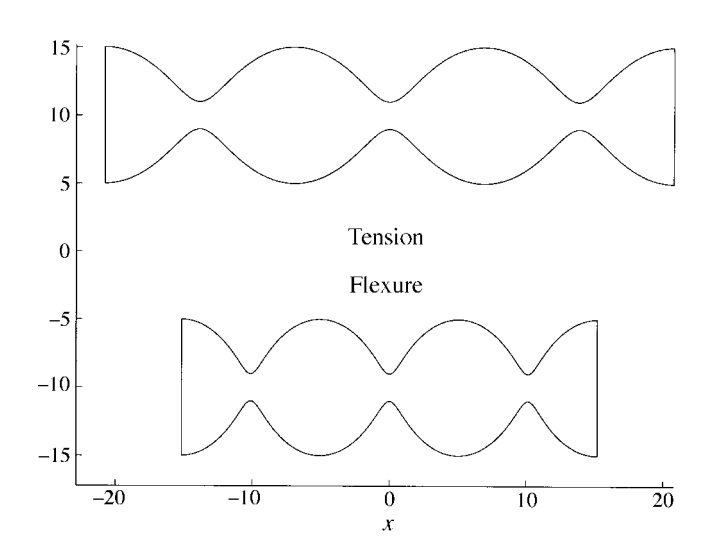


Fig. 5 The equilibrium shapes for tension (top) and flexure (lower) for the same values of $a_2/a_1 = 5$ and $\Lambda_0 = 0.3$

numerically harmless by parametrizing a and x in terms of θ as follows:

$$a(\theta) = \frac{1}{2}(a_2 + a_1) + \frac{1}{2}(a_2 - a_1)\sin\theta, \qquad -\frac{1}{2}\pi \leqslant \theta \leqslant \frac{1}{2}\pi,$$

$$x(\theta) = \int_{-\frac{1}{2}\pi}^{\theta} d\theta \cos\theta \left[\frac{1}{(1 - \Lambda_0 g(\theta)\cos^2\theta)^2} - 1 \right]^{-\frac{1}{2}}, \qquad -\frac{1}{2}\pi \leqslant \theta \leqslant \frac{1}{2}\pi, \tag{63}$$

where

$$g(\theta) \equiv \frac{1}{\Lambda_0} \left. \frac{(a_2 - a_1)^2 G(a)}{4(a_2 - a)(a - a_1)} \right|_{a = a(\theta)}.$$
 (64)

It may be readily verified that the function $g(\theta)$ is positive and bounded away from zero for $\theta \in [-\frac{1}{2}\pi, \frac{1}{2}\pi]$. In particular it is non-zero at $\theta = \pm \frac{1}{2}\pi$, and hence the integral in (63) can be easily computed.

Some examples of the equilibrium shapes are displayed in Figs 3 to 5. These are based upon the equations for a and x in (63), where x is found by expressing it as an ordinary differential equation for $x(\theta)$ and then using a Runge–Kutta routine. The shapes in Fig. 3 represent small values of Λ_0 , relative to the critical value defined by the constraint (60), whereas the shapes in Fig. 4 are at the critical value. At this value of Λ_0 the slope becomes vertical at the point of inflection a_0 , and the vertical slope is apparent in Fig. 4. The maximum slope is smaller for the lower values of Λ_0 in Fig. 3. Also, we note that the length in the x-direction becomes larger the smaller the value of Λ_0 . This scaling follows from the explicit appearance of Λ_0 in (63); the function $g(\theta)$ is independent of Λ_0 , and in the limit of small Λ_0 we therefore have

$$x(\theta) = \frac{1}{\sqrt{\Lambda_0}} \int_{-\frac{1}{2}\pi}^{\theta} \frac{d\theta}{\sqrt{2g(\theta)}}, \quad -\frac{\pi}{2} \leqslant \theta \leqslant \frac{\pi}{2}, \quad \text{for } \Lambda_0 \ll 1.$$
 (65)

For instance, for the tension loading we find that (65) can be solved in closed form as

$$x(\theta) = \frac{4}{\sqrt{\Lambda_0}} \left(\frac{a_2}{a_1} - 1 \right) \left(\frac{a_2}{a_1} \right)^{1/4} E\left(\frac{\pi}{4} + \frac{\theta}{2}, i\sqrt{\frac{a_2}{a_1} - 1} \right), \quad -\frac{\pi}{2} \leqslant \theta \leqslant \frac{\pi}{2}, \quad \text{for } \Lambda_0 \ll 1,$$
(66)

where E is the incomplete elliptic integral of the second kind (17). In general, the length in the x-direction scales as $\Lambda_0^{-1/2}$, and we will use this scaling in the subsequent analysis.

Finally, Fig. 5 compares the equilibrium shapes under tensile and flexural loading. In general, numerical experiments indicate that the shapes do not differ much, whether the loading is tensile or flexural.

5. Nonlinear evolution of symmetric configurations

5.1 The governing equation

We now turn to the nonlinear evolution of a plate from an initially perturbed configuration, relative to a flat state. Only symmetric systems are considered, and we again assume that the elastic strain energy is given by the simplified uni-dimensional static solutions of (43) for the two distinct types of loading.

We consider a plate of finite extent: $0 \le x \le l$ where l is the length of a specimen, or the length of the unit cell for an infinitely long but periodic system. Arclength on the surface satisfies $ds/dx = (1 + (a_{,x})^2)^{1/2}$, and therefore, the rate of change in the surface height is related to c via the kinematic relation

$$\partial a/\partial t = (1 + (a_x)^2)^{1/2} c$$
. (67)

Referring to equations (10) and (45), the evolution equation for a becomes

$$\frac{\partial a}{\partial t} = D_0 \frac{\partial}{\partial x} \left[\frac{1}{\sqrt{1 + (a_{,x})^2}} \frac{\partial}{\partial x} \left(\bar{U}(a) - \frac{\gamma a_{,xx}}{\left(1 + (a_{,x})^2 \right)^{3/2}} \right) \right], \quad 0 \leqslant x \leqslant l, \quad 0 < t,$$
 (68)

supplemented by initial data for a(x, t). A linear stability analysis of this equation, with $a = a_0 + h$ and h given by (18), yields the growth rates of (40), in agreement with the theory for finite ka in the thin-plate limit.

The total free energy of the plate system follows from (1) with

$$E_{\text{elastic}} = \int_0^l dx \int_{-a}^a dz \, \frac{\sigma_{11}^2}{2E_p}, \qquad E_{\text{surface}} = \int ds \, 2\gamma. \tag{69}$$

The stress $\sigma_{11}(z,t)$ is independent of z and equal to $F_0/(2a)$ for tension, but depends upon z for flexural loading, according to $\sigma_{11} = M_0 z/I$ with $I = \frac{2}{3}a^3$. The factor of 2 in E_{surface} arises from the two surfaces. The work done by the applied end loads is

$$W = F_0[u]$$
 for tension, $W = M_0[w]$ for flexure, (70)

where [u] = u(l,t) - u(0,t) is the difference in the horizontal displacement between the two ends, and $[w_{,x}]$ is the corresponding jump in the rotation, defined by the derivative of the transverse deflection w. Using

$$[u] = \int_0^l dx \, \epsilon_{11}, \qquad [w_{,x}] = \int_0^l dx \, w_{,xx},$$
 (71)

combined with the relations $\epsilon_{11} = F_0/(2aE_p)$ for tension and $w_{,xx} = M_0/(E_pI)$ for flexure, and expressing ds in (69)₂ in terms of x, we finally arrive at an expression for the free energy:

$$\mathcal{E} = \int_0^l dx \left(\int_{-a}^a dv \bar{U}(v) + 2\gamma \sqrt{1 + (a_{,x})^2} \right). \tag{72}$$

The expression (72) is useful because we will evaluate the free energy later and demonstrate that it does actually decrease with time.

Define the non-dimensional variables X, T and A by

$$x = lX, t = \frac{l^4 T}{D_0 \gamma}, a = a_0 A, (73)$$

where a_0 now represents a typical thickness, for example, the initial semi-thickness. The present theory is essentially a thin-plate approximation, since we are using thin-plate solutions for the strain energy, and it is appropriate to define a thinness parameter:

$$\epsilon \equiv a_0/l. \tag{74}$$

The governing equation (68) can be expressed in terms of the non-dimensional variables by using $a_{,x} = \epsilon A_{,X}$, etc. Substituting for $\bar{U}(a)$ from equation (43), we obtain

$$\frac{\partial A}{\partial T} = \frac{\partial}{\partial X} \left[\frac{1}{\left(1 + \epsilon^2 (A_{,X})^2\right)^{1/2}} \frac{\partial}{\partial X} \left(\frac{\Lambda_0}{2\epsilon^2 A^m} - \frac{A_{,XX}}{\left(1 + \epsilon^2 (A_{,X})^2\right)^{3/2}} \right) \right], \quad 0 \leqslant X \leqslant 1, \quad 0 < T,$$
(75)

where m is an integer,

$$m = \begin{cases} 2 & \text{in tension,} \\ 4 & \text{in flexure,} \end{cases}$$
 (76)

and Λ_0 is a non-dimensional ratio of strain to surface energy:

$$\Lambda_0 = \frac{\sigma_0^2 a_0}{\gamma E_p} \,. \tag{77}$$

Here, σ_0 is the stress at $a = a_0$ according to the thin-plate elasticity theory, and we note that Λ_0 is the same non-dimensional parameter that persistently occurs (see (28) and (57)). The non-dimensional chemical potential and free energy follow from (4)₂, (43) and (72) as

$$\bar{\mu} = \epsilon^2 \left[\frac{\Lambda_0}{2\epsilon^2 A^m} - \frac{A_{,XX}}{\left(1 + \epsilon^2 (A_{,X})^2\right)^{3/2}} \right], \quad \text{where } \bar{\mu} = \frac{a_0 \mu}{\gamma}, \tag{78}$$

and

$$\bar{\mathcal{E}} = \int_0^1 dX \left(\sqrt{1 + \epsilon^2 (A_{,X})^2} - \frac{\Lambda_0}{2(m-1)A^{m-1}} \right), \quad \text{where } \bar{\mathcal{E}} = \frac{\mathcal{E}}{2\gamma l}.$$
 (79)

5.2 Thin-plate approximation

In order to be consistent with the thin-plate theory we should limit the application of the uniaxial approximation to plates with small surface slopes, or equivalently to ones for which the horizontal length scale for variation in thickness far exceeds the thickness itself. Hence, $\epsilon \ll 1$. At the same time, the analysis of the previous section indicated that the length in the *x*-direction scales with $1/\sqrt{\Lambda_0}$ when Λ_0 is small, see (65) and (66). Hence, to be fully consistent $\sqrt{\Lambda_0}$ should be of the same order as ϵ , and their ratio is of order unity. In summary, we assume the scalings

$$\epsilon \ll 1, \qquad \Lambda_0 \ll 1, \qquad \lambda = O(1), \tag{80}$$

where λ is a rescaled O(1) version of Λ_0 :

$$\lambda \equiv \Lambda_0 / \epsilon^2. \tag{81}$$

Consequently, (75) can be replaced by its leading-order approximation in ϵ :

$$\frac{\partial A}{\partial T} = \frac{\partial^2}{\partial X^2} \left(\frac{\lambda}{2A^m} - \frac{\partial^2 A}{\partial X^2} \right), \quad 0 \leqslant X \leqslant 1, \quad 0 < T.$$
 (82)

This is the governing evolution equation for thin plates. The associated chemical potential is of order ϵ^2 , from equation (78),

$$\bar{\mu} = \epsilon^2 \left[\frac{\lambda}{2A^m} - A_{,XX} \right]. \tag{83}$$

The corresponding non-dimensional free energy follows from (79), after adding a constant,

$$\bar{\mathcal{E}} = \frac{\epsilon^2}{2} \int_0^1 dX \left[\left(\frac{\partial A}{\partial X} \right)^2 - \frac{\lambda}{(m-1)A^{m-1}} \right], \tag{84}$$

and the rate of change of the free energy is therefore, using (9) and (83),

$$\frac{d\bar{\mathcal{E}}}{dT} = -\frac{\epsilon^2}{2} \int_0^1 dX \left[\frac{\partial}{\partial X} \left(\frac{\lambda}{2A^m} - \frac{\partial^2 A}{\partial X^2} \right) \right]^2. \tag{85}$$

5.3 Numerical examples and analysis

It does not appear to be feasible to obtain closed-form solutions to the canonical evolution equation (82), so we resort to numerical methods. We consider the domain $0 \le X \le 1$, and assume periodic boundary conditions, that is A(X,T) and its derivatives with respect to X are the same at X=0 and X=1. Equation (82) is solved numerically on a spatial grid (X_j,T_n) , with $X_j=j\Delta X$, $j=1,2,3,\ldots,N$ where $X_N=1$, and $T_n=n\Delta T$, using a semi-implicit scheme for each time step. Thus, the values $A_j^n \ (\approx A(X_j,T_n))$ are marched forward in time according to the scheme, for $n\to n+1$,

$$A_{j}^{n+1} + \frac{\Delta T}{2(\Delta X)^{4}} \left(A_{j+2}^{n+1} - 4A_{j+1}^{n+1} + 6A_{j}^{n+1} - 4A_{j-1}^{n+1} + A_{j-2}^{n+1} \right)$$

$$= A_{j}^{n} - \frac{\Delta T}{2(\Delta X)^{4}} \left(A_{j+2}^{n} - 4A_{j+1}^{n} + 6A_{j}^{n} - 4A_{j-1}^{n} + A_{j-2}^{n} \right) + \frac{\Delta T}{(\Delta X)^{2}} \left(f_{j+1}^{n} - 2f_{j}^{n} + f_{j-1}^{n} \right), \tag{86}$$

where $f_j^n = \lambda/[2(A_j^n)^m]$. The differencing for the linear fourth-order operator is semi-implicit, removing the constraint of a very small time step. The size of the time step is selected to comply with the Lax stability criterion for the linear second-order differencing scheme.

An analysis of the linearized version of equation (82) for A near unity,

$$A_{.T} + m\lambda A_{.XX} + A_{.XXXX} = 0, (87)$$

with $A(X, T) = 1 + \widetilde{A} \exp{\{\nu T + i K X\}}$ implies that

$$v = (m\lambda - K^2)K^2. \tag{88}$$

The quantity ν is clearly the non-dimensional analog of η as given by equation (40). The most unstable wavenumber is $K = (m\lambda/2)^{1/2}$ with linear exponential growth $\nu = m^2\lambda^2/4$.

For example, Fig. 6 illustrates the time evolution of a unit period of a plate for the initial profile $A(x,0)=1+\delta\sin(2\pi x)$, with $\lambda=8\pi^2/m$ and $\delta=-0.3$. The progression to zero thickness speeds up steadily, and consequently, in order to show the ultimate behaviour the curves in Fig. 6 do not represent equal time steps. The actual rate of thinning is clear from Fig. 7 which shows the minimum thickness as a function of time step. Note that the time steps were different in the two simulations, because it takes far longer for the tensile notch to develop. It is clear that the thinning occurs first relatively slowly, until the notch is well defined. Then, as $T \to T_*$, where T_* is the time at which A vanishes, the thinning progresses rapidly, and is highly localized near the point of final failure at $X=X_*$.

We also checked that the total free energy, $\bar{\mathcal{E}}$ of (84), is a monotonically decreasing function. In fact, its decrease is similar to that for the thickness: first slow, then becoming more rapid as $T \to T_*$. Also, the numerical results indicate that $\bar{\mathcal{E}}$ approaches a finite value for tension/compression, but that it tends to negative infinity for flexure.

We can gain some insight into the behaviour indicated in Figs 6 and 7 by a scaling argument valid for the inner region where the rapid thinning occurs as $T \to T_*$. Thus, let $X - X_* = (T_* - T)^{\alpha} y$, $A(X,T) = (T_* - T)^{\beta} \lambda^{\gamma} F(y)$. Then requiring that all three terms in (84) contribute implies that $\alpha = 1/4$ and $\beta = 1/[(2(m+1)]]$. By the further choice of $\gamma = 1/(m+1)$ we obtain an equation for F which is independent of λ . In summary, the scaling yields

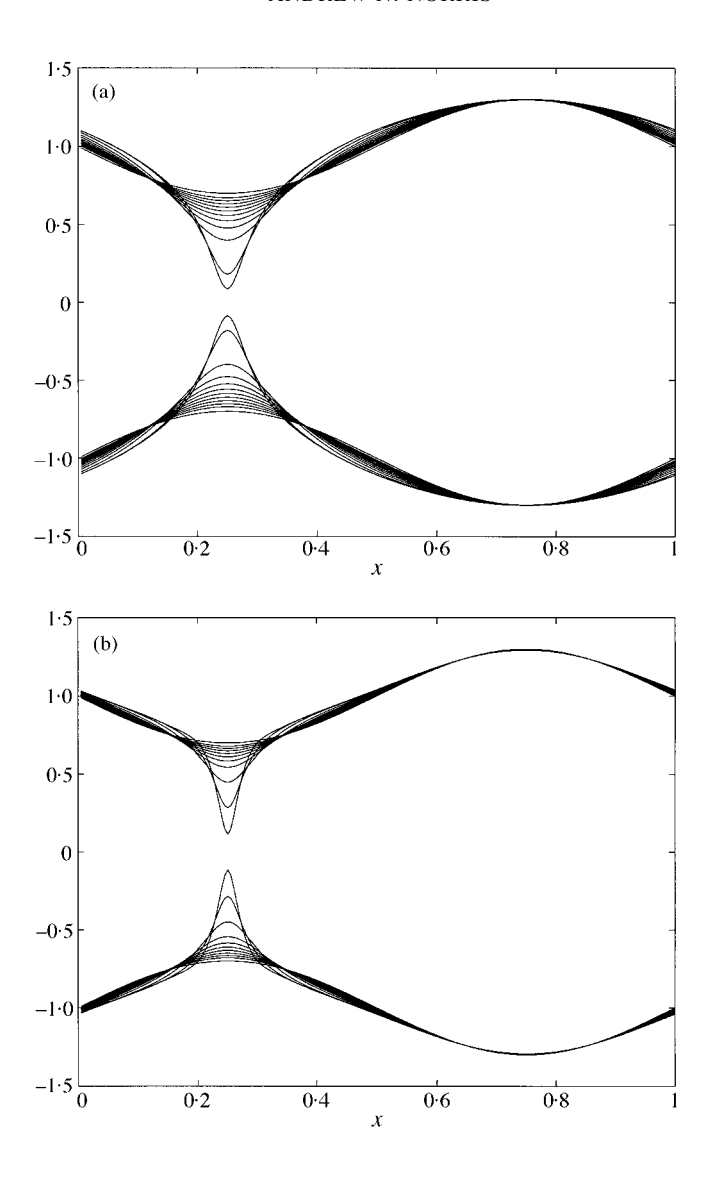
$$A(X,T) \approx \lambda^{1/(m+1)} \left(T_* - T \right)^{1/2(m+1)} F\left((X - X_*)(T_* - T)^{-1/4} \right), \qquad X \to X_*, \quad T \to T_*,$$
(89)

where the function F(y) satisfies an ordinary differential equation,

$$F'''' - \frac{1}{2} \left(\frac{1}{F^m} \right)'' + \frac{y}{4} F' - \frac{F}{2(m+1)} = 0, \quad -\infty \leqslant y \leqslant \infty.$$
 (90)

The solutions of (90) should be symmetric in y, and therefore only $0 \le y < \infty$ needs to be considered. This requires four conditions, two of which are, from symmetry, F'(0) = 0 and F'''(0) = 0. The other two are obtained by requiring that for large $(X - X_*)$ the solution become independent of T. This is a consequence of the observation that far from the thinning region the thickness is essentially constant. Assuming a power law scaling: $F(y) \sim y^p$, $y \to \infty$, implies that p must be p = 2/(m+1). Therefore the remaining pair of conditions are that

$$\lim_{y \to \infty} y^{-2/(m+1)} F(y) = \rho, \qquad \lim_{y \to \infty} y^{(m-1)/(m+1)} F'(y) = \frac{2}{m+1} \rho \tag{91}$$



 $\textbf{Fig. 6} \quad \text{The evolution of a plate under (a) tension/compression and (b) flexure. The initial and subsequent shapes are depicted}$

ELASTIC PLATES 305

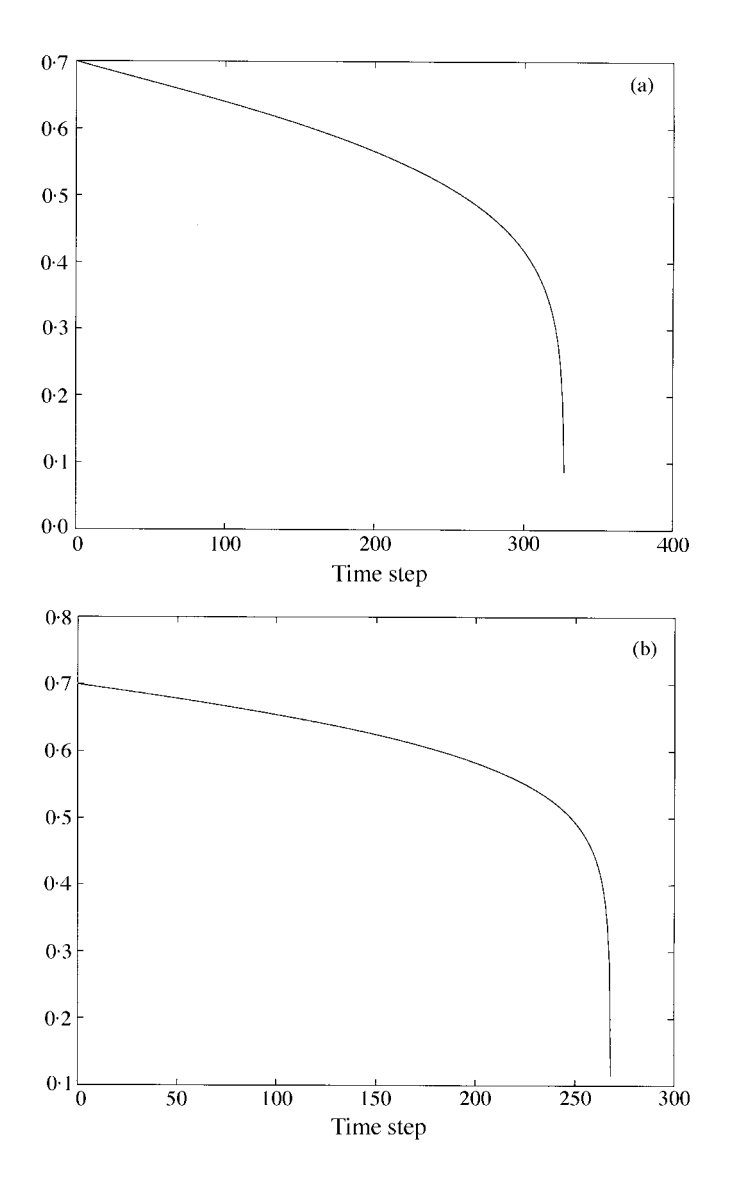


Fig. 7 The evolution of the minimum thickness for the simulations of Figure 6: (a) tension/compression and (b) flexure

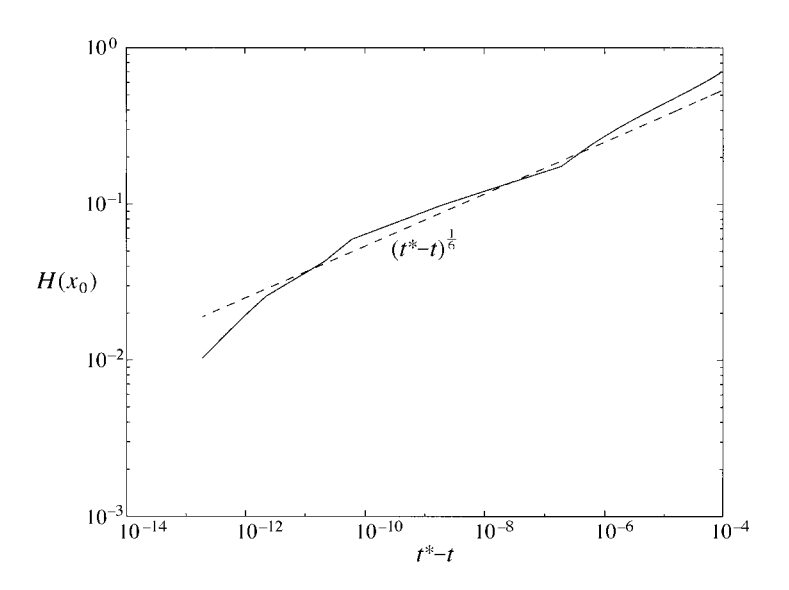


Fig. 8 A comparison of the numerically computed minimum thickness for tension/compression (solid curve) with the inner scaling according to equation (92)

for some $\rho > 0$.

Regardless of the precise nature of the F functions, the scaling (89) indicates that the minimum thickness of the notch behaves like

minimum thickness
$$\sim$$

$$\begin{cases} (T_* - T)^{\frac{1}{6}} & \text{in tension} \\ (T_* - T)^{\frac{1}{10}} & \text{in flexure} \end{cases}$$
 (92)

Figure 8 shows the minimum thickness for tension/compression loading versus $(T_* - T)$, where T_* is estimated by extrapolation from curves like those in Fig. 7. The agreement in Fig. 8 indicates that the inner scaling does indeed take over at late times.

The scaling argument implies that the change in the total free energy is caused by the thinning region alone, and it can therefore be estimated from (89). Thus, equation (84) gives

$$\bar{\mathcal{E}} = \frac{1}{2} \epsilon^2 \lambda^{2/(m+1)} \left(T_* - T \right)^{(3-m)/4(m+1)} I_m, \quad T \to T_*, \tag{93}$$

where the constant I_m is

$$I_{m} = \int_{-\infty}^{\infty} dy \left[\left(F' \right)^{2} - \frac{1}{(m-1)F^{m-1}} \right], \tag{94}$$

while the rate of change of the free energy is, using (85),

$$\frac{d\bar{\mathcal{E}}}{dT} = -\frac{\epsilon^2}{2} \lambda^{2/(m+1)} \left(T_* - T \right)^{-(5m+1)/4(m+1)} J_m, \quad T \to T_*, \tag{95}$$

where

$$J_m = \int_{-\infty}^{\infty} dy \left[\left(F'' - \frac{1}{2F^m} \right)' \right]^2. \tag{96}$$

Comparing equations (94) and (96) implies the identity

$$J_m = \frac{3-m}{4(m+1)} I_m \,, \tag{97}$$

and hence $I_2 > 0$, $I_4 < 0$ because $J_m > 0$. It is interesting to note that the energy for the plate in tensile loading decays to zero, while the energy of the flexurally loaded plate tends to negative infinity, that is,

$$\bar{\mathcal{E}} \sim \begin{cases} \epsilon^2 \left(T_* - T \right)^{\frac{1}{12}} & \text{in tension} \\ -\epsilon^2 \left(T_* - T \right)^{-\frac{1}{20}} & \text{in flexure} \end{cases}$$
 (98)

Of course, the energy cannot decrease indefinitely for the plate in flexure. The safety net is provided by the constraint that the above estimates are for the leading-order asymptotic theory, for which the energy of the system is $O(\epsilon^2)$. Hence, the estimates of (95), for example, are valid as long as $\bar{\mathcal{E}}$ remains of order ϵ^2 , but they fail once $\bar{\mathcal{E}}$ becomes $O(\epsilon)$ or larger.

6. Discussion

The equilibrium and evolution equations for thin plates were derived from the general theory for elastic solids under the simplifying approximation of uniaxial stress. This essentially eliminated stress from the problem and rephrased the mechanics entirely in terms of the thickness as the fundamental parameter. In retrospect, one can recast the theory for thin elastic plates in a relatively simple form. Thus, the free energy follows from (72) as

$$\mathcal{E} = \int_0^l dx \, V(a, a_{,x}), \tag{99}$$

where V follows from (43) and (72) as

$$V(a, a_{,x}) = \begin{cases} -\frac{F_0^2}{4E_p a} + 2\gamma \sqrt{1 + (a_{,x})^2} & \text{in tension,} \\ -\frac{3M_0^2}{4E_p a^3} + 2\gamma \sqrt{1 + (a_{,x})^2} & \text{in flexure.} \end{cases}$$
(100)

The two conditions that mass be conserved and that the free energy be non-increasing, that is,

$$\int_0^l dx \, a = \text{constant} \qquad \text{and} \quad \frac{d\mathcal{E}}{dt} \leqslant 0 \,, \tag{101}$$

are then sufficient to determine the form of the growth law. Thus, mass is maintained if the normal velocity is the surface derivative of a function:

$$c = -\partial q/\partial s. (102)$$

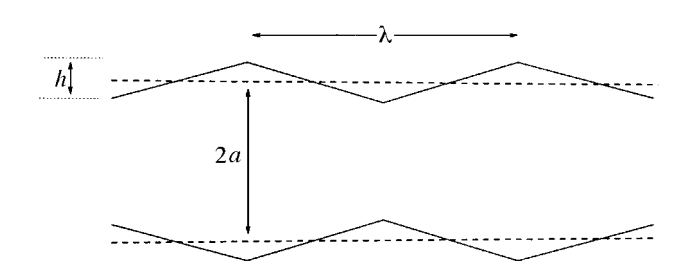


Fig. 9 The thin-plate stability criterion can be understood by means of this simplistic perturbation combined with the uniaxial approximation

The free energy is then a monotonically decreasing quantity if the function q satisfies

$$q = -D_0 \frac{\partial}{\partial s} \left(\frac{\partial V}{\partial a} - \frac{\partial}{\partial x} \frac{\partial V}{\partial a_{,x}} \right), \qquad D_0 > 0.$$
 (103)

Using (67), this leads directly to the evolution equation in the form

$$\frac{\partial a}{\partial t} = D_0 \frac{\partial}{\partial x} \left[\frac{1}{\sqrt{1 + (a_x)^2}} \frac{\partial}{\partial x} \left(\frac{\partial V}{\partial a} - \frac{\partial}{\partial x} \frac{\partial V}{\partial a_x} \right) \right], \quad 0 \leqslant x \leqslant l, \quad 0 < t, \tag{104}$$

which is identical to (68).

As a final point we note that the uniaxial theory also permits a relatively simple stability argument. Consider the perturbed plate in Fig. 9. As the thickness changes the stress maintains a constant resultant force

$$\sigma(x) = \frac{2a\,\sigma_0}{2a + 2\delta(x)}.\tag{105}$$

For simplicity we take $\delta(x)$ as piecewise linear with average zero of one period of length λ :

$$\delta(x) = \left[\frac{h}{2} - \frac{2h}{\lambda} \left| |x| - \frac{\lambda}{4} \right| \right] \operatorname{sgn}(x), \qquad -\frac{\lambda}{2} \leqslant x \leqslant \frac{\lambda}{2}.$$

The change in free energy per unit period is thus

$$\Delta \mathcal{E} = -\frac{\lambda h^2}{12a} \frac{\sigma_0^2}{2E_p} + 4\frac{h^2}{\lambda} \gamma. \tag{106}$$

This yields a critical wavenumber at which $\Delta \mathcal{E}$ vanishes, $\lambda = (4/\sigma_0)(6a\gamma E_p)^{1/2}$. The more detailed analysis for a sinusoidal perturbation yields, in the appropriate thin-plate limit, from (40), a wavelength $\lambda_{\text{max}} \equiv 2\pi/k_{\text{max}}$ equal to $(2\pi/\sigma_0)(2a\gamma E_p)^{1/2}$, which differs by about 10 per cent from the simple estimate based upon Fig. 9.

7. Conclusions

Starting from the linear stability analysis of a plate of finite thickness relative to the wavelength of the perturbation, we have shown that the limit of a thin plate exhibits quite different behaviour

ELASTIC PLATES 309

than a thick plate, or a half-space. The fundamental difference is that the whole structure—the thin plate—supports the stress and the variations in the stress. This observation permits a simple uniaxial approximation which allows us to eliminate the stress in favour of the plate thickness as the fundamental variable. It simplifies considerably the nonlinear equilibrium and non-equilibrium mechanics of thin plates.

We have derived for the first time equilibrium shapes of thin plates for either tensile/compression or flexural loading. These are characterized by surfaces with constant chemical potential. The nonlinear evolution of thin plates under stress-driven surface diffusion has also been analysed for the first time. Two distinct regimes were found, similar to the observations of Yang and Srolovitz (5) for the plane-strain half-space problem. First, there is a steady but slow growth of an initial surface disturbance. The thinning subsequently speeds up, reaching zero thickness in finite time. The behaviour near the ultimate breakage of the plate can be described by an inner scaling which predicts a universal power law for the thickness as a function of time before 'failure'. The numerical and analytical results also indicate that flexural loading leads to a more rapid and a more catastrophic failure

Thin-plate configurations are of fundamental significance in modern technology, particularly in small structural components. The results presented for equilibrium configurations indicate that certain shapes are preferable for avoiding or delaying diffusion-driven instability, and could have implications in the design of nano-scale devices. The quasi-static evolution to failure can also be modelled by the simple uniaxial theory presented here. This provides some understanding of stress-driven instability leading to fracturing, and it may serve as a starting point for analysing more complex configurations.

Acknowledgement

This work was supported by the Office of Naval Research.

References

- **1.** R. J. Asaro and W. A. Tiller, *Metall. Trans.* **3** (1972) 1789–1796.
- 2. M. A. Grinfeld, Sov. Phys. Dokl. 31 (1986) 831–835.
- 3. D. J. Srolovitz, Acta Metall. 37 (1989) 621–625.
- 4. L. B. Freund, Int. J. Solids Struct. 32 (1995) 911–923.
- 5. W. H. Yang and D. J. Srolovitz, Phys. Rev. Lett. 71 (1993) 1593–1596.
- **6.** K. Kassner and C. Misbah, Europhys. Lett. **28** (1994) 245–250.
- 7. B. J. Spencer and D. I. Meiron, Acta Metall. Mater. 42 (1994) 3629–3641.
- 8. R. H. Torii and S. Balibar, J. Low Temp. Phys. 89 (1992) 391–400.
- 9. D. K. Tappin, I. M. Robertson and H. K. Birnbaum, Acta Mater 44 (1996) 735–746.
- **10.** M. A. Tenan, O. Teschke and M. U. Kleinke, *Langmuir* **6** (1990) 1640.
- 11. J. R. Rice and T.-J. Chuang, J. Am. Cer. Soc. 64 (1981) 46–53.
- **12.** J. Tersoff and F. K. LeGoues, *Phys. Rev. Lett.* **72** (1994) 3570–3573.
- 13. A. N. Norris, Int. J. Solids Struct. 35 (1998) 5237-5252.
- 14. Z. Suo, Adv. appl. Mech. 33 (1997) 193-293.
- **15.** W. W. Mullins, *J. appl. Phys.* **28** (1957) 333–339.
- **16.** I. S. Sokolnikoff, *Mathematical Theory of Elasticity* (Krieger 1983).
- **17.** I. S. Gradshteyn and I. M. Ryzhik, *Tables of Integrals, Series and Products* (Academic Press, London 1980).